Chapter 12

Characterizations of Environmental Composites

Ali Hammood and Zainab Radeef

Additional information is available at the end of the chapter

http://dx.doi.org/10.5772/50494

1. Introduction

Recently, environmental preservation issues have been critical between the chemical pollution matters and the development technology requirements. However, the renewable and friendly materials come to use.

Numerous researches have richly studies the natural fiber reinforcement polymer composites. This fact, based on both fibers and matrixes are derived from renewable resources. Therefore, the formed composites have more compatibility with the environmental preservation issues. [1] Isabel investigated of the most natural fibers are used such as palm, cotton, silk, coconut, wool and wood fibers. A significant development in the lignocelluloses fiber in thermoplastics realized the distinct researches presented by [2-5] Composite-reinforcing fibers can be categorized by chemical composition, structural morphology, and commercial function. Natural fibers, such as kenaf, ramie, jute, flax, sisal, sun hemp and coir are derived from plants that used almost exclusively in PMCs. Aramid fibers [6] are crystalline polymer fibers are mostly used to reinforce PMCs. The compounds percentage of composite have the essential role for verify the designed values according to applications, therefore the mechanical properties of PMCs predicated by Mohamed (2007).

The primary function of a reinforcing fiber is to increase the strength and stiffness of a matrix material. The fibers reinforced composite have the essential role in this investigation for its significant property advantages as high stiffness, lightweight, easily recycled material, availability, low manufacturing cost, the environment effect and lifetime rupture behavior. Various types of natural fibers are available to combine with other mineral fiber for construct composite material. Essentially, the fiber can be classified as vegetable, animal, and man-made fibers. The main disadvantages of natural fibers are their high level of moisture absorption, poor and interfacial adhesion, relatively low heat resistance. [7-8] investigated high speed impact events using (PKV, PRM) composites. This research was indicated significant improvements in the penetration resistance. This fact comes from the improvement of target geometry structure. Numerous researches have been carried out on

the ballistic impact on high strength fabric structures [9-11]. In the airport and marine applications, the dynamic loads effect and the chemo interactions were attracted the researchers and many methods are employed for computing the surface topography parameters, thereby numerous estimations were covered the erosion-corrosion behavior of PMCs [12-13]. The most impinging parameters focused on environment effects and impinging angle [14-17]. There were many instruments and electronic microscopes developed with the time for measuring the roughness parameters and drawing the surface topography [19]. The Erosion and corrosion of composite must be determent for the accelerator objects, whereby this values will be indicator for measuring the life time rupture of composite [18].

2. Important

The automotive and aerospace industries have both shifted for using natural fiber reinforced composites as a factor to reduce the weight and getting significant properties of composite components. As matter of fact, the impinging liquids of the naval and aerospace applications have a direct effect on surface topography. Therefore, advanced studies focused on corrosion and erosion behavior. The impinging angle, velocity versus time, composite morphology represented the essential parameters of this field of study. In this investigation, surface roughness versus time was the indicator for erosion and corrosion effects.

3. Experiment Procedure and Samples Preparation

In order to develop new composite material with high impact resistance and high erosion resistance, characterization study for two sets of composites materials have been computed. The specific composites materials in this research are: polyester resin-matrix and Kevlar reinforced fiber (PKV) with V_f (42%), polyester resin–matrix and ramie reinforced fiber (PRM) with V_f (42%). Experimental program was carried out to study the erosion and corrosion behavior by computing the surface roughness parameters of (PKV, PRM) before and after impinging operation. Hence, Polymer Matrix Composites (PMCs) were examined by impingement using water jets when the aqueous solution was 3.5 wt% NaCl. Erosion and corrosion tests were impinging at 90 angles at velocity 30 m/s and the impinging period was 12 hours.

The composite subject study consists from five Kevlar layers and five ramie layers were impregnated with unsaturated polyester. The layers aligned alternatively according to the expectation performance. The synthetic ramie fiber was weaved as shown in Figure 1(a) & (b).

4. Tensile testing of composites

Tensile specimen (145 x 15 x 7) mm3 are caught according to ASTM D 3039 /D 3039M-95M standard (ASTME D 3039, 2003). Tensile test has been conducted and the data acquired digitally. Tensile stress, tensile strain and Young modulus of PKV with Vf (42%) and PRM with Vf (42%) were calculated and the test was performed by instron machine 10 KN, series

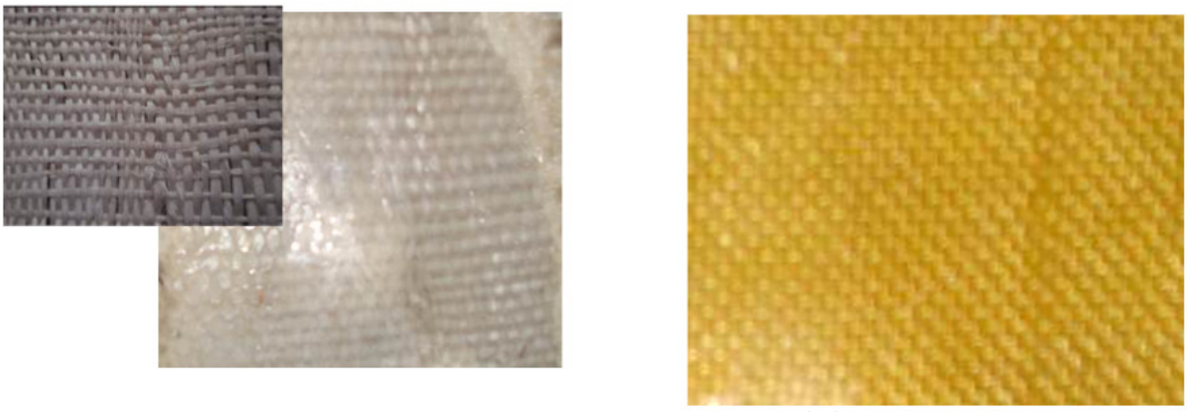

(a) Ramie Woven and PRM (b) Kevlar Woven

Figure 1. Ramie and Kevlar Woven

2716 and 2736 under stable speed rate 2 mm/min. The test has verified all the specific test conditions to determine the tensile properties of specimen according to the ISO 527. Tensile test has been performed to estimate the yield stress, young modulus and tensile extension at yield point. Additionally, Poisson's ratio has been calculated by evaluate transverse strain and longitudinal strain of composite. Hence, the transverse strain calculated by using strain gage that supplied from Tokyo Sokki Kenkyuio co, Ltd. The used gage type was BFLA-2-8 with gage resistance 120±0.3 Ω. Then, the strain is connected to DAQ bridge system for reading the transverse strain.

The composite behavior under test was an important subject for this investigation and the specimen geometry was constructed from five layers Ramie fiber and five layers of Kevlar as clarified in the Figure 2.

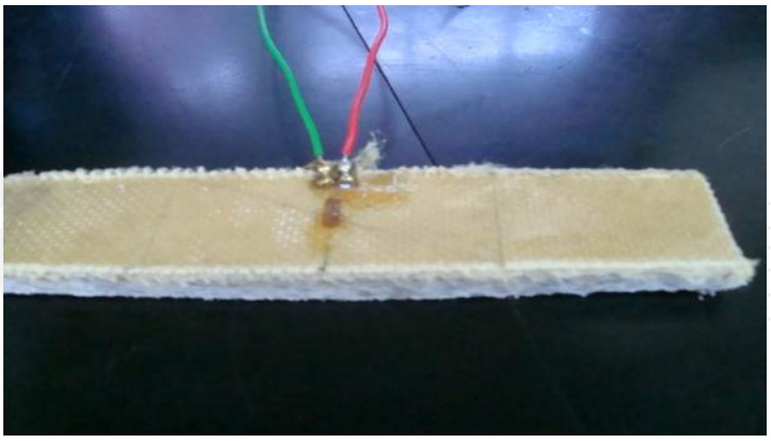

Figure 2. Tensile Test Specimen with Strain Gage

5. Ballistic limit and number of layers

The ballistic limit is commonly defined as a 50% probability of penetrating a target at a given impact velocity. The energy absorption is related to the impact velocity, interpreted by the effect of the striking velocity on the amount of kinetic energy that is absorbed by the

composite material. Hence, the energy absorbed by the fabric is equal to the residual energy amount subtracted from total impact energy.

In this test, the target impinged by using gas gun machine supported by a high speed camera for record the impact event at 30,000 frames per second with image size 512 x 64 pixels per image [7]. Figure 3 (a) shown the gas gun machine. Thus, The velocity before the target and the residual velocity after the target were estimated. All the targets were impinged by Semi-conical bullets as shown in the Figure 3(b).

(a) Ballistic Panel

(b) Semi-conical bullets

Figure 3. Gus gun device of University Putra Malaysia [7,8]

6. Erosion test and corrosion

Accurate estimation is carried out for calculating the erosion and corrosion percentage of (PKV, PRM) samples. The tests were conducted using a jet at velocity 30 m/s and impinging angles 90°. Essentially, the exposure period was the major factor of erosion estimation. Hence, the impinging periods were from 3 to 6 and from 6 to 12 hours under room temperature. Samples roughness data were recorded before and after the tests by Image processing software for scanning probe microscope

7. Result and discussions

7.1. Tensile test

The tensile test of this composite was conducted for specifying the mechanical properties of the composite. Generally, the test results recorded high tensile strength. The brittle manner was the first stage of composite under test due to the low elongation ability of matrix. The second stage was the ductile behavior that embodied of high elongation ability of Kevlar layer. From stress – strain curve topography, the specimen have extension at maximum load up to 2.49 mm was recorded. There are continuously reductive of the curve as a result to the elongation of Kevlar layers. The extension at maximum tensile strain observed at 43.25 mm that was evident in the ductile behavior at front face of the specimen. Practically, through

the extension test, the back face of the specimen that contented from ramie layers reinforced polyester was separated gradually as result to the brittle behavior of ramie – polyester matrix. Automatic Young's modulus in this composite is 4930.5 MPa. This fact plotted in stress – strain curve in the Figure 4. The composite properties depend at compounds types and volume fraction. Therefore, the volume fraction of fiber or matrix could be calculated as it is clarified in the following equation.

$$V_m = \frac{\nu_m}{\nu c} \tag{1}$$

Where

V_m = volume fraction of matrix

ν_m = volume of matrix

ν_c = total volume of the composite

Volume fraction of fiber could be evaluated from.

$$V_m = 1 - V_f \tag{2}$$

Where

V_f = volume fraction of fiber

The volume of ramie fiber could be calculated from the following equation.

$$V_f = V_K + V_R \tag{3}$$

Where

V_k = volume fraction of Kevlar

V_R = volume fraction of ramie

Fiber density can be determined experimentally by weighting the Kevlar and ramie fibers and calculated the volume fraction for the fibers and resin. Therefore, from the following expression could be calculated the density.

$$\delta_f = \frac{\delta_c - V_m \delta_m}{V_f} \tag{4}$$

Where

δ_f = Fiber density

δ_c = Composite density

δ_m = Matrix density

The Poisson coefficient represents the contraction in the transverse direction and could be calculated by using the follow expression.

$$V_{lt} = v_f V_f + v_m V_m \tag{5}$$

$$V_{lt} = 0.34 \tag{6}$$

V_{lt} = Poisson ratio

Where the Kevlar Poisson ratio is equivalent to 0.34 [6], ramie Poisson ratio is equal to 0.3 [20] and 0.4 for unsaturated polyester resin [21].

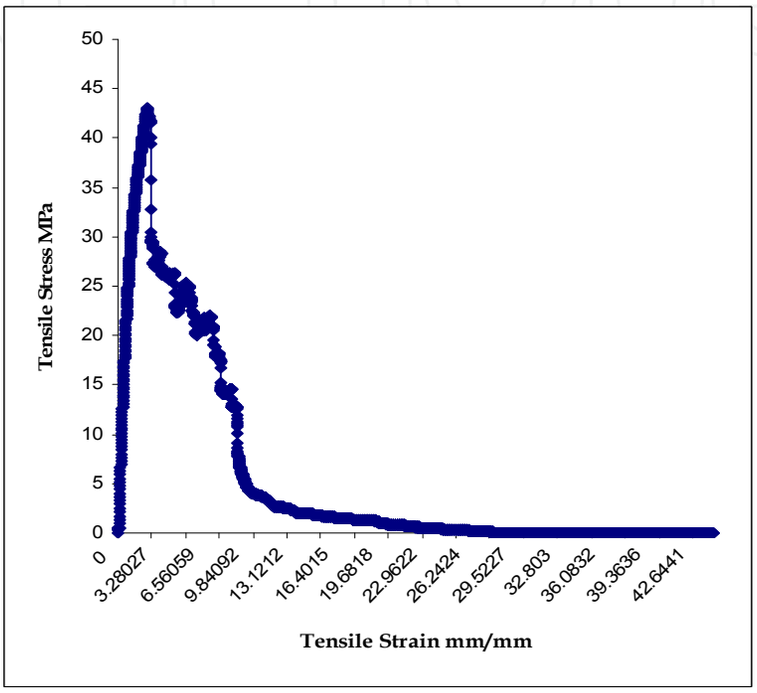

Figure 4. Stress – Strain Curve of PKV +PRM Composite

Modulus of elasticity (E_{11}) can be calculated in (7).

$$E_{11} = \frac{\sigma_L}{\varepsilon} \tag{7}$$

σ_L =longitudinal tensile stress
ε =strain

(E_{22}) is calculated by using gage strain that recorded the shrinking displacement and more than 550 data point recorded load and displacement. The transverse Young's Modulus is the initial slope of σ_{tra}. ε_2 curve.

The Young's modulus can be calculated by using the retrieved data from Figure 5 as clarified in the following equation.

$$E_{22} = \frac{\sigma_{tra}}{\varepsilon_2} \tag{8}$$

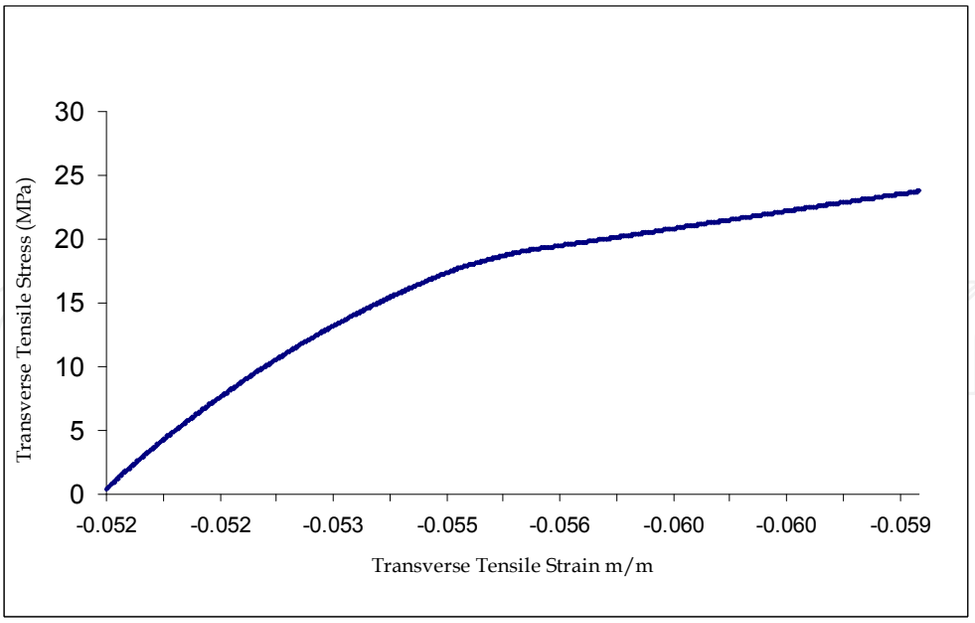

Figure 5. Stress – Transverse Tensile Stress and Strain Curve of Composite

Where

E_{22} = Transverse Young's Modulus

σ_{tra} =Transverse tensile stress

ε_2 = Transverse strain

The maximum shear stress can be obtained from the following equation.

$$\tau_{max} = \frac{\sigma_y}{2} \tag{9}$$

Where

σ_y = Stress in the yield point

τ_{max} = Maximum shear stress

Shear modulus (G_{12}) can be calculated from the load data that plotted in the shear stress curve.

$$G_{12} = \frac{\tau}{\gamma} \tag{10}$$

Where

τ = shear stress

γ = shear strain

In addition, the Poisson ratio can be estimated from the following equation and the result seems equivalent to the Poisson ratio that was calculated according to the compounds volumes fraction. Table 1 presents the longitudinal and transverse averages of data.

$$\gamma_{12} = \frac{\varepsilon_{lat}}{\varepsilon_{long}} \tag{11}$$

Where

ε_{lat} =Transverse strain

ε_{long} =Longitudinal strain

The average of longitudinal data for Kevlar – Ramie –Polyester composite				
E_{11} (GPa)	$(\sigma_1)_{ult}$ (MPa)	$(\varepsilon_1)_{ult}$	ζ_{max} (MPa)	Poisson's Ratio
3.9489±0.5	66.75±5.4	0.125±0.04	33.37±3	0.37

The average of transverse data for Kevlar – Ramie –Polyester composite				
E_{22} (MPa)	$(\sigma_2)_{ult}$ (MPa)	$(\varepsilon_2)_{ult}$	γ_{12}	G_{12} (MPa)
244.74±2.5	22.77±1.3	0.0735±0.03	0.257±0.05	132.65±15

Table 1. Tensile Test Data

7.2. High speed impact results

Understanding the impact response of composites has be come an area of great academic and practical interest. The major advantages of composite materials are their high strength and stiffness, light weight, corrosion resistance, crack, fatigue resistance and flexibility. Ramie – Kevlar reinforced polyester resin present high resistance. The high level from resistance could be realized by increasing of Kevlar layers.

$$[E_{abs} = \frac{1}{2} m \ \ (V_{imp}^2 - V_{res}^2)] \tag{12}$$

Where

E_{abs} = Energy absorption

m = projectile mass

V_{imp} = Impact velocity

V_{res} = Residual velocity

Ballistic limit can be identified as the limit between the penetration and the fully arrested. Thus, the composite with five layers (PKV) and five layers (PRM) couldn't meet the specific requirements of ballistic resistance. In fact, the absorption of energy will be increased with increase the number of layers [7, 8].

In the event when no perforation occurs, the energy absorbed by the target will be equal to the initial impact energy. The high speed impact data for PKV & PRM are shown in the table 2. The following equation has been verified to the ballistic limit or fully arrested action.

$$[E_{abs} = \frac{1}{2} m \quad V_{imp}^2] \tag{13}$$

Where
E_{abs} = absorption of energy
V_{imp} = impact velocity

In this prospective must be mention the most high speed impact parameters that represented rich fields of studies are, target geometry, projectile type, target thickness, composite compounds.

Humanity:53%	Bullet type: Semi-conical
Specimen type: TSP	Camera temperature:40 °C
Target area:15 × 10 mm	Temperature: 32 °C
Material: PKV& PRM	Camera resolution: 512 × 48

Layer No.	Gas gun Pressure Psi	Initiation Velocity m/s	Residual velocity m/s	Absorption of Energy J
5K-5R	300	273.9	125.9	147.926
	250	275.255	150.17	133.035
	250	255.07	120.9	126.109

Table 2. High Speed Impact of PKV & PRM

7.3. Erosion result

The surface roughness of engineering applications has interacted with the environment. Therefore, the studies pay attention for estimating the surfaces roughness of materials with respect to essential parameters to limit the wear mechanism of materials. Roughness value can either be calculated on a profile or on a surface Rz, Rq, and Sa is the arithmetic average of the 3D roughness. Hence, the impinging test conduct through specific periods is illustrated in the Table (3).

Kevlar roughness by (nm)				Ramie roughness by (nm)			
0 hours	3 hours	6 hours	12 hours	0 hours	3 hours	6 hours	12 hours
8.92	11	9.36	9.94	12.9	11	6.71	10.8
16.7	8.25	8.06	10.4	7.37	9.82	6.85	10.4
15.6	8.44	7.94	11	10	8.32	7.78	10.3
7.53	9.26	6.35	8.78	9.12	11	7.82	8.43
6.06	8.69	6.24	11.6	10.6	10.9	8.25	8.8
6.44	12.9	9.45	10.4	11.3	8.31	9.23	9.18
6.28	12.9	8.81	14	10.6	11.3	9.97	9.57

Table 3. Roughness values

The roughness parameters rates, such as (Amplitude parameters, Hybrid Parameters and Functional Parameters) were estimated by all morphology images with image size (100.00nm X 80.00nm) Figure 6 illustrate the morphology images before PKV tests.

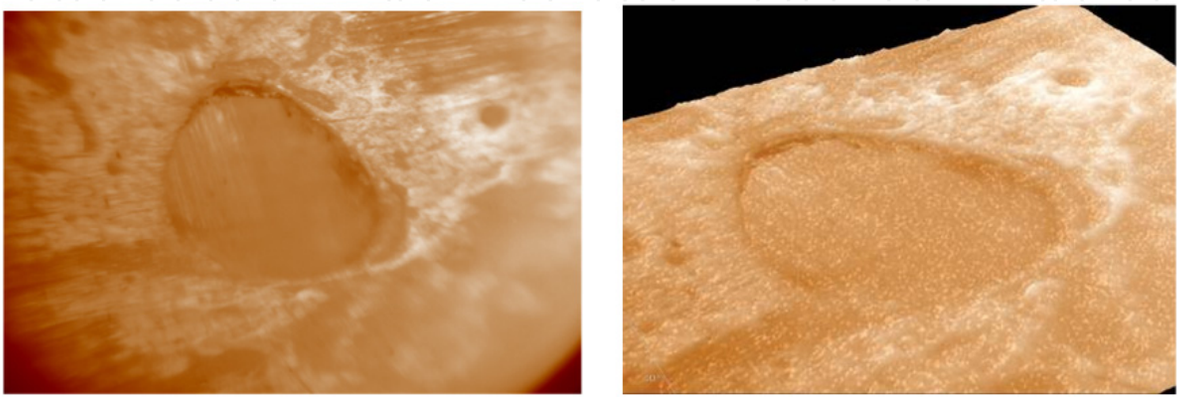

Figure 6. 3D Morphology Images after Tests of PKV.

The erosion wear loss was determined using probe microscope. Typically, scanning probe microscope image process software provided reliable means to evaluate the erosion volume lose. This technique characterizes and quantifies the surface roughness parameters, the surface profile and topographical features in three-dimension using high precision range observed at 100 nm. All measurements were made with an effective magnification of X 12.5. Excellent data were recorded for average size and average height for surface grains. Hence, the average volume of grains can be computed by the grain size analyzer. Randomly, erosion areas were elected for scanning morphologic image. The erosion volume loss was derived from analyzing the erosion surface at three dimensions. Therefore, the erosion volume loss (Vloss) can be expressed as the average volume of surface at zero erosion time (V0) subtracted from the average volume of surface after specific time (Vt). Eroded area was randomly measured at seven locations. Then, the average of erosion volume was calculated.

$$V_{loss} = V_0 - V_T \tag{14}$$

According to the V_{loss} formula, the averages of erosion volume loss were illustrated in Figure 7.

Ramie reinforced polyester matrix present higher value of volume erosion loss than Kevlar reinforced polyester. This fact derives from the poor of adhesion between Kevlar filaments and polyester resin. Table 4 illustrates the grains size versus time.

volume loss	Kevlar			Ramie		
	avg. size (nm^2)	avg. height (nm)	avg. volume	avg. size (nm^2)	avg. height (nm)	avg. volume
Zero Time	1.13	7.14	8.21	1.24	8.97	11.18
after 3 hours	1.11	10.334	10.44	0.82	9.36	7.846
after 6 hou	1.72	8.91	11.55	0.9	5.41	4.25.003

Table 4. Grains size versus time

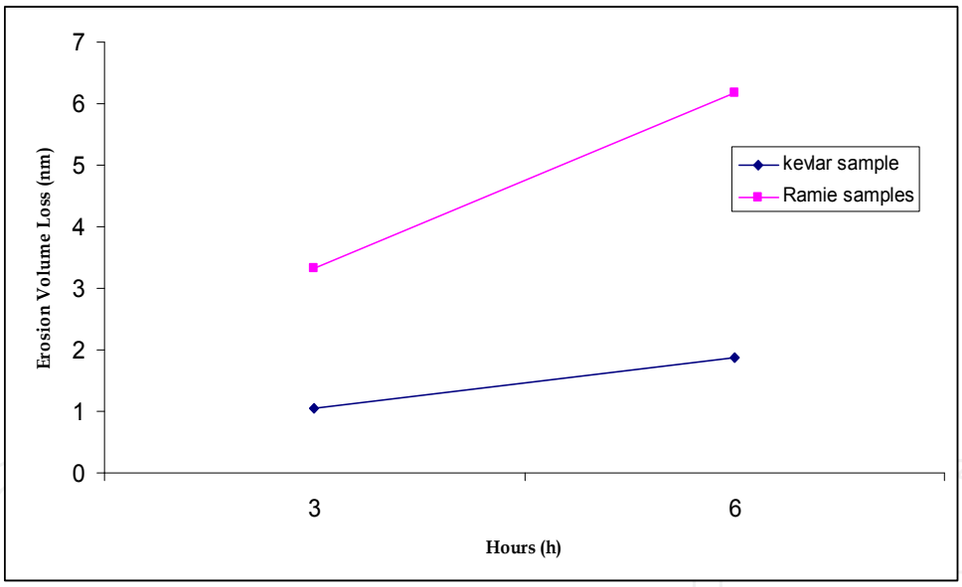

Figure 7. Erosion volume loss concomitant with time

Transforming image to 3D topography with 200% zoom area for PKV sample at zero time (before test) illustrated accurate 3D surface profile with 243 peaks number and the maximum height 46 nm as shown in the Figure 8 and Figure 9 shown the PKV after 12 hours illustrated in 3D surface with 238 peaks number and maximum height 73.6 nm.

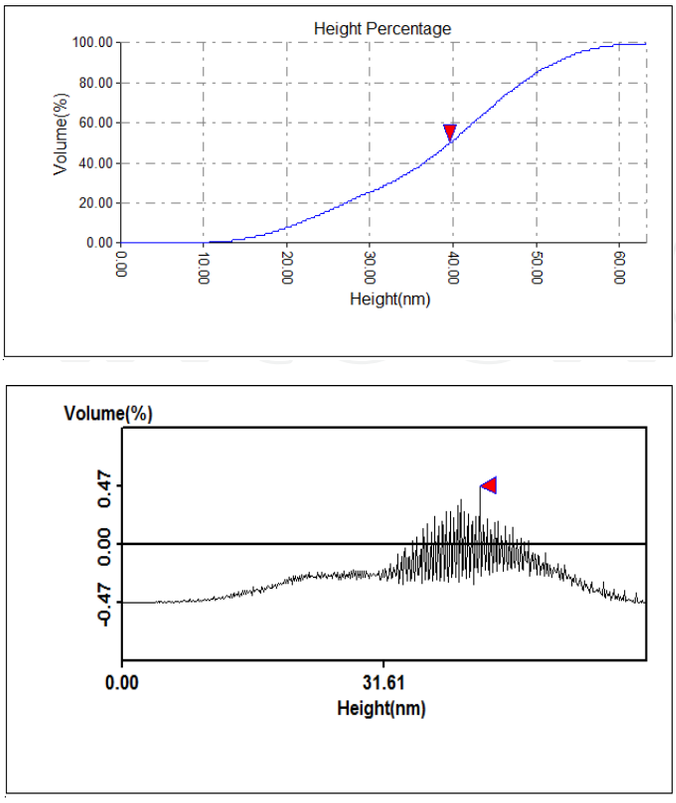

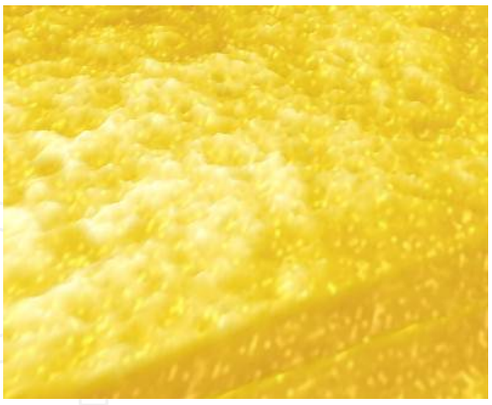

Figure 8. PKV at Zero Time (before test) in 3D Image

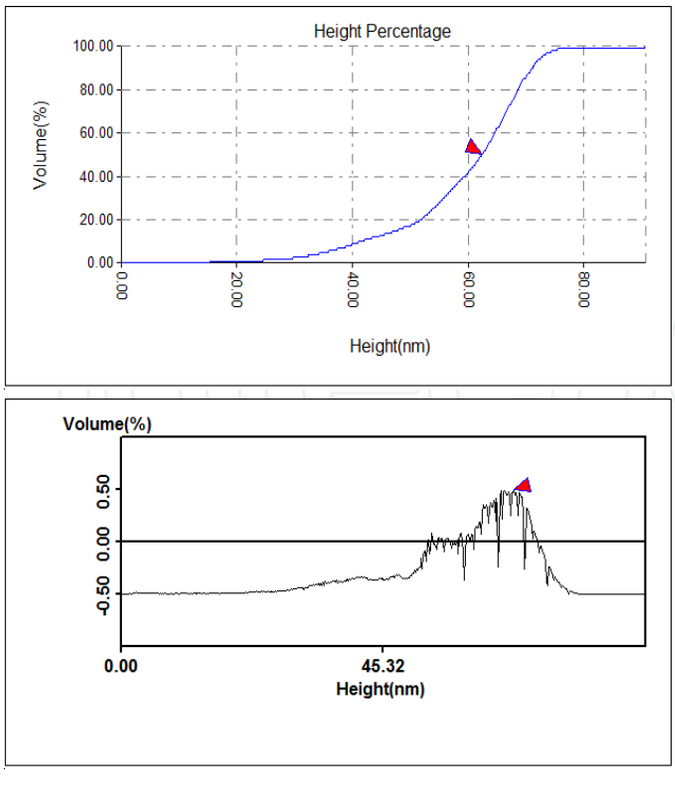

Figure 9. PKV after 12 Hours in 3D Image

Accurate roughness parameters were established for PKV and PRM versus the time before and after test as illustrates in the table 5. PKV & PRM morphologies images versus time were illustrated in Figure 10 & 11.

Image size:100.00nm X 80.00nm (PKV) at zero time					
Amplitude parameters:	Area 1	Area 2	Area 3	Area 4	Area 4
Sa(Roughness Average) [nm]	6.06	7.53	8.92	15.6	16.7
Sq(Root Mean Square) [nm]	9.1	10.7	12.3	18.8	20.2
Ssk(Surface Skewness)	-2.32	-1.67	-1.58	-0.451	-0.386
Sku(Surface Kurtosis)	12.7	8.92	6.75	2.41	2.44
Sy(Peak-Peak) [nm	87.8	90.2	89.5	90.3	91.4
Sz(Ten Point Height) [nm]	85.2	89	85.8	89.9	88.5
Hybrid Parameters:					
Ssc(Mean Summit Curvature) [1/nm]	-155	-161	-146	-146	-149
Sdq(Root Mean Square Slope) [1/nm]	10.1	10.7	8.12	8.69	8.02
Sdr(Surface Area Ratio)	3.29E+03	3.62E+03	2.17E+03	2.44E+03	2.08E+03
Functional Parameters:					
Sbi(Surface Bearing Index)	0.624	1.05	0.779	2.45	14.1
Sci(Core Fluid Retention Index)	0.983	1.18	0.949	1.34	1.32
Svi(Valley Fluid Retention Index)	0.192	0.17	0.211	0.103	0.112
Spk(Reduced Summit Height) [nm]	4.79	7.41	4.61	7.98	0.355
Sk(Core Roughness Depth) [nm]	16.4	20.1	22.4	44.4	55.1
Svk(Reduced Valley Depth) [nm]	21.5	20.8	25.2	19.9	19.6
Sdc 0-5(0-5% height intervals of Bearing Curve) [nm]	14.6	10.2	15.7	7.67	1.43
Sdc 5-10(5-10% height intervals of Bearing Curve)[nm]	1.72	3.08	1.31	4.32	0.803
Sdc 10-50(10-50% height intervals of Bearing Curve) [nm]	7.63	9.69	10.3	19.4	26.9
Sdc 50-95(50-95% height intervals of Bearing Curve) [nm]	16.6	19.9	26	36.1	35.7
Spatial Parameters:					
Sds(Density of Summits) [1/um2]	4.28E+06	4.23E+06	6.02E+06	5.67E+06	5.56E+06
Fractal Dimension	3	3	2.81	2.37	2

Table 5. The roughness parameters rates

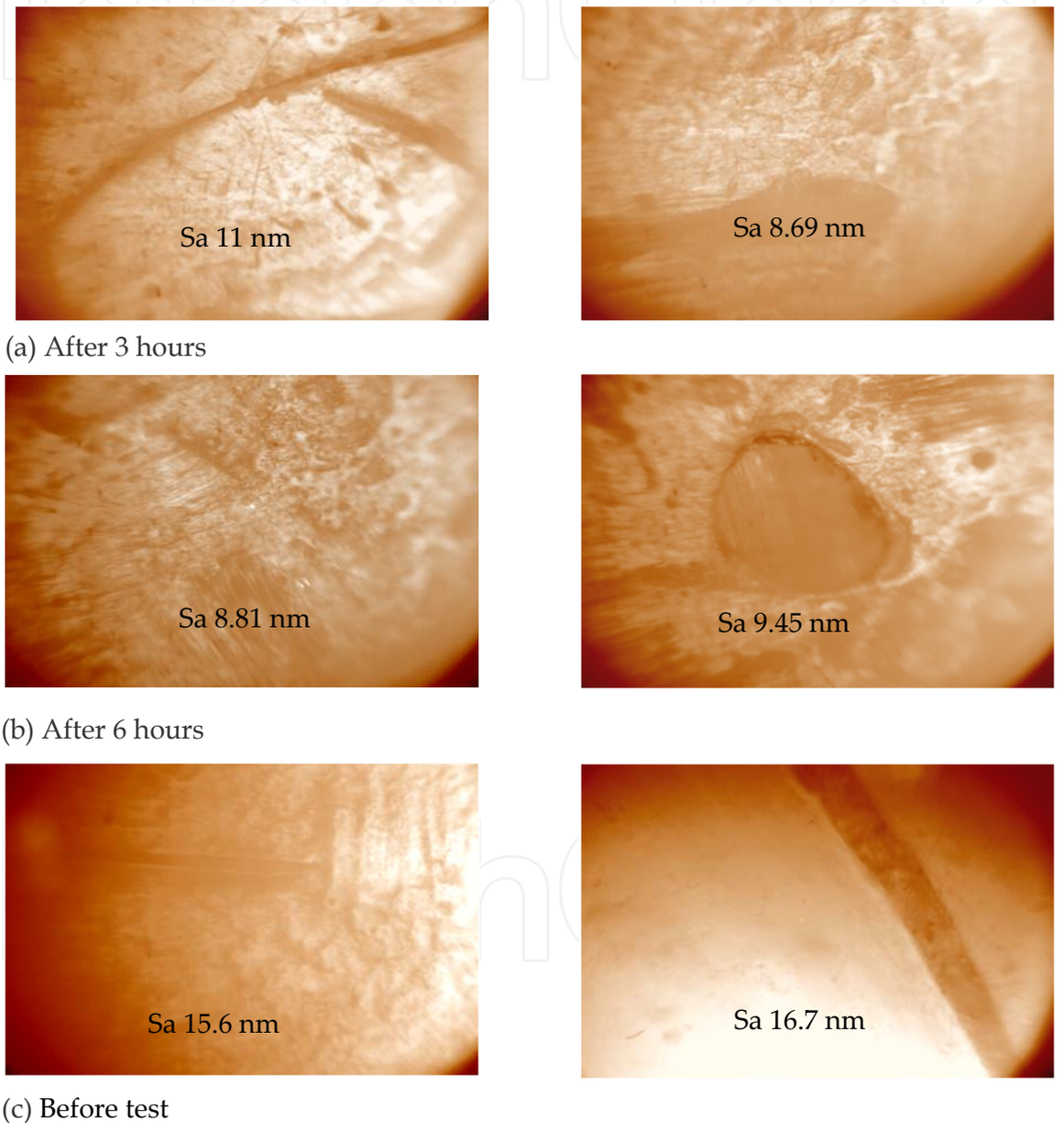

Figure 10. Erosion and corrosion test for Kevlar – polyester composite morphology and Sa(Roughness Average)

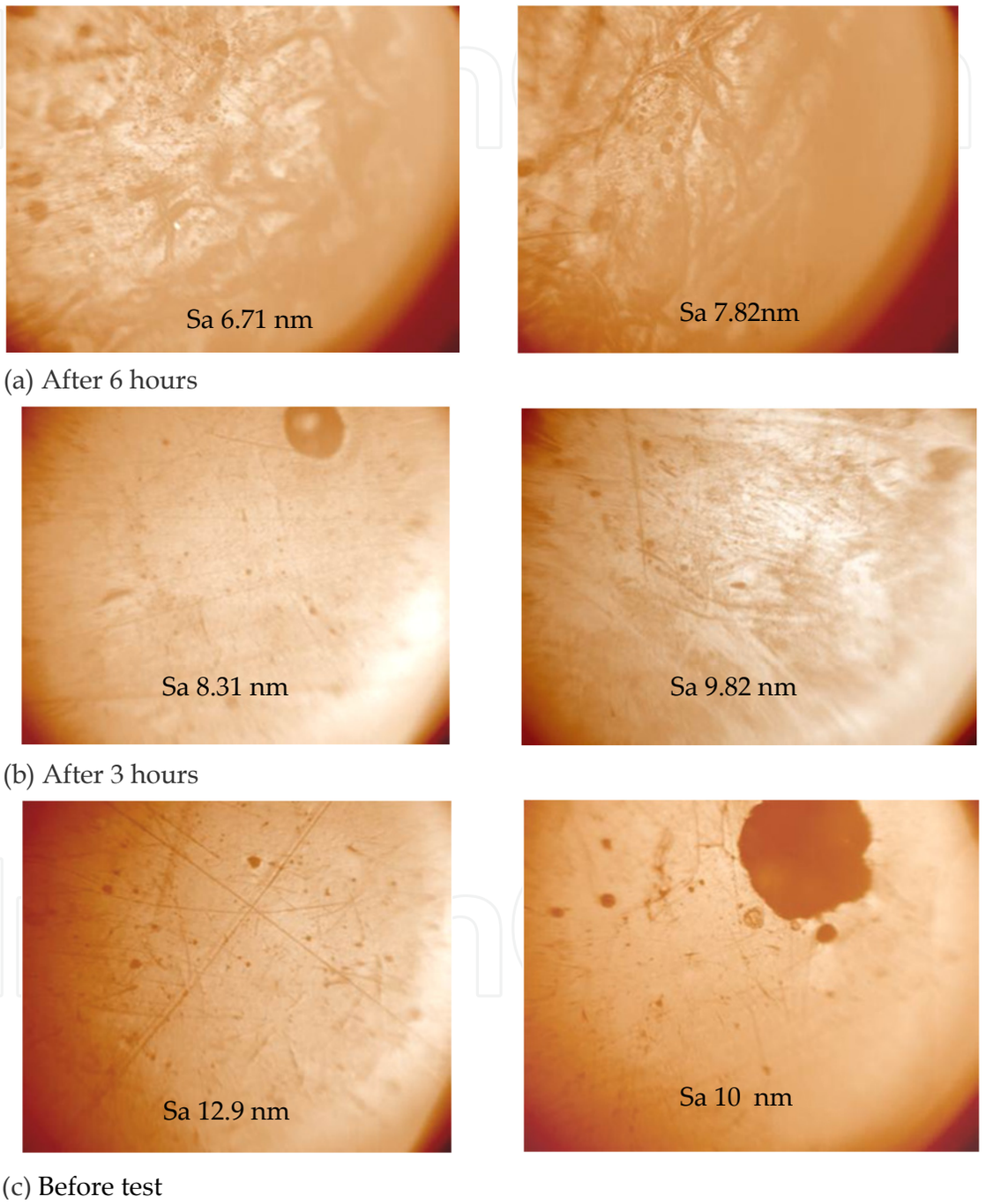

Figure 11. Ramie – polyester composite morphology and Sa(Roughness Average) after erosion-corrosion test

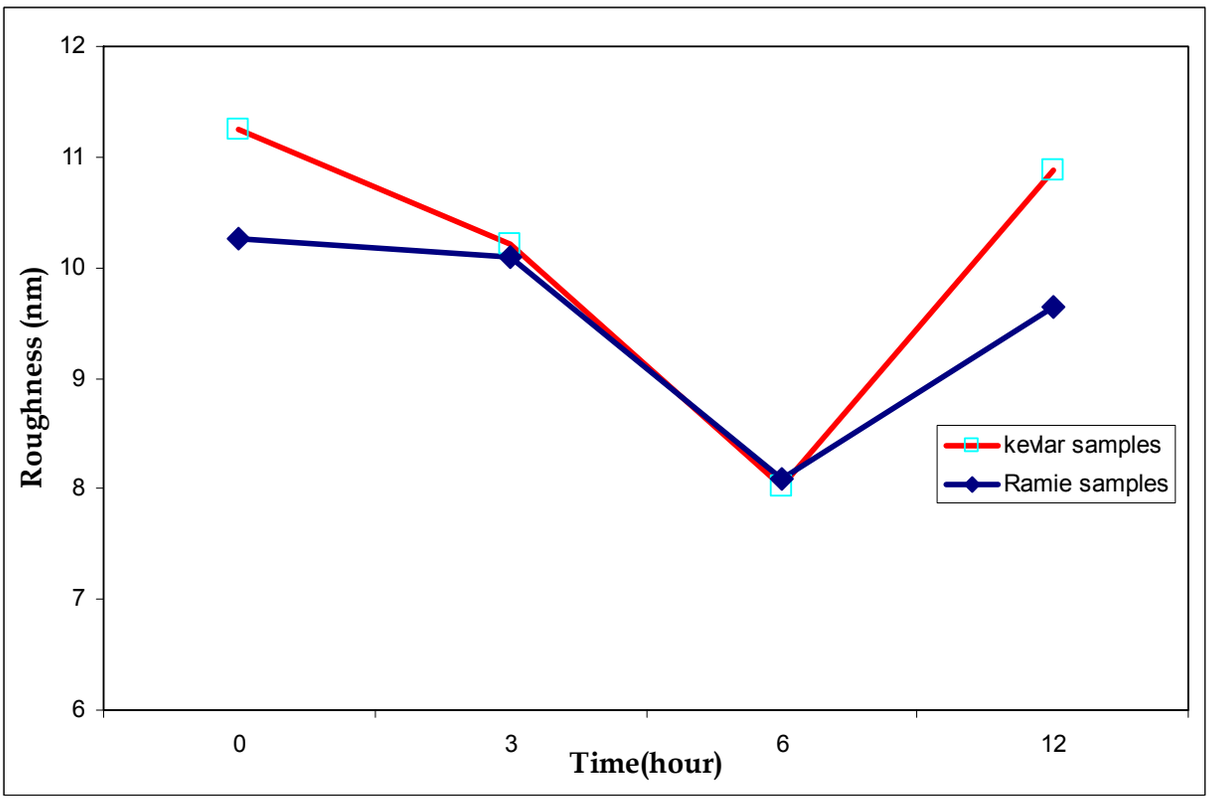

Figure 12. The Roughness Rates Versus Time

The roughness rate of the Kevlar–polyester and ramie-polyester concomitant time tented to be equivalent values. Really, the polyester reinforced faced the impinged water has the major role in the erosion and corrosion resistance. The Kevlar and ramie fibers have specific interfacial adhesion with the matrix. The ramie fibers presented high interfacial adhesion with resin as a result to plant fiber nature. On the other hand, the Kevlar presented a poor linkage with polyester resin.

All the fiber layers were protected by the matrix mass. Figure12 illustrated a declining in the polyester surface roughness versus time. The roughness will be the function for estimating the erosion rate. Therefore, within the period, from 3 until 6 hours the impinging effect assisted of soften the surface, but within period from 6 until 12 hours the erosion rate will be increase and the surface tent to be rough. Electrochemical test have been conducted and there are no significant corrosion data recorded, this finding derived from the compound nature of composite.

8. Conclusions

Generally, plain weave represented the most common fabric, due to the significant properties that embodied their tensile strength to weight ratio. The study of the stress – strain response, high speed impact evaluation, and erosion corrosion behavior leads to the following conclusion:

1. The Kevlar –polyester composites behave ductile manner but the ramie-polyester composites behave brittle manner.
2. The roughness rate of the Kevlar-polyester and ramie-polyester decreases through 3 -6 hours but there is an increase in the roughness rate through 6-12 hours due to the increasing in erosion rate of polyester matrix.
3. All roughness parameter computed accurately.
4. PKV and PRM with five layers PKV and five layers PRM present fully penetration.
5. No significant corrosion has been recorded.

Author details

Ali Hammood and Zainab Radeef
Department of Materials Engineering-University of Kufa, Iraq

Acknowledgement

The authors would like to express their gratitude and sincere appreciation to the department of Mechanical and Manufacturing Engineering of the University Putra Malaysia and Material Engineering Department- College of Engineering-University of Kufa for scientific assistance and support.

9. References

[1] Isabel B Wingate (1976) Textile fabrics and their selection. Library of congress cataloging in publication data.
[2] Woodhams R T, Thomas G, Rodgers D K (1984) wood Fiber as Reinforcing Fillers forpolyolefins.polym.eng.Sci. Vol(24):1166.
[3] Klason C, Kubat J (1989) Cellulose in polymer composites. In composite Systems from Natural and synthetic polymers, Salmen L, de Ruvo, A Sefe-ris, J C Stark, E B Eds; Elsevier Science: Amsterdam
[4] Myers G E, Clemons C M, Balatinecz J J, Woodhams R T(1992) Effects of composite and polypropylene Melt Flow on polypropylene-Waste Newspaper Composites. proceedings on the Annual Technical Coneference; Society of plastics Industry p 602
[5] Kokta, B V, Raj R. G, Daneault C (1989) Use of Wood Flour as Filler in Polypropylene; Studies on Mechanical Properties. Polymplast. Tecnol.Eng. 28, 247.
[6] Yang H H (1993) Kevlar Aramid Faiber. west Sussex PO191UD,England.
[7] Aidy A, Shaker Z R, Kahalina A (2010) Development of anti-ballistic board, fiber polymer-plastics technology and engineering VOL.(50):622-634.
[8] Zainab Shaker Radif, Aidy Ali & Khalina Abdan(2010) DEVELOPMENT OF A GREEN combat armour from rame-kevlar- polyester composite, Pertanika Journal of Science and Technology. Vol(19) : PP 339-348,.
[9] Lee B L, Song J W, Ward J E J (1994) Compos Mater.VOL (28):PP 1202 – 1226.

[10] Goldsmith W, Dharan CK.,Chang H (1995) Quasi-static and ballistic perforation of carbon fiber laminates .Int J Solid Struct VOL(32):89-103.
[11] Almohandes AA, Abdel – Kader MS, Eleiche, AM (1996) Experimental investigation of the ballistic resistance of steel-fiberglass reinforced polyester laminated plates. Composites: Part B 27:447-58.
[12] Bardal E, Eggen T G, Rogne T, Solem T (1995) The erosion and corrosion properties of thermal spray and other coatings, in: Proceedings of the Int. Therm. Spray. Conf., Kobe, Japan.
[13] Puget Y, Tretheway K R,Wood R J K (1998) The performance of cost effective coatings in aggressive saline environments, NACE Corrosion PP 688.
[14] Burstein G T, Sasaki K (2000) Effect of impact angle on the slurry erosion–corrosion of 304 L stainless steel, Wear VOL (240): 80–94.
[15] Dawson J L, Shih C C, John C C, Eden D A (1987), Electrochemical testing of differential flow induced corrosion using jet impingement rigs, NACE Corrosion, Paper no. 453,.
[16] Clark H M, Wong K K, Impact angle (1995), particle energy and mass loss in erosion by dilute slurries, Wear 186–187 454–464.
[17] Stack M M, Zhou S, Newman R C, Identifications of transitions in erosion–corrosion regimes in aqueous environments, Wear 186 (1995) 523–532.
[18] Sherrington.(1988), modern measurement techniques in surface metrology, wear VOL(125):271-288.
[19] Matsuno Y., Yamada H., Harada M. and Kobayashi A. (1975), The microtopography of the grinding wheel surface with SEM, Ann.CIRP VOL(24):PP 237-242.
[20] Nakamura, Y et al (2003). Neurosci. Abst. 608.5
[21] Girardi M. A and Phill M. G. (1993), Microstructure and properties of polyester/urethane acrylate thermosetting blends, and their use as composite matrices, Journal of Materials Science, Volume 28. 3116-3124, DOI: 10.1007/BF00354718.
[22] Mohamed Thariq. (2007), High velocity Impact analysis of glass epoxy-laminate plates. Thesis, university Putra, Malaysia, Malaysia.